$YBa_2Cu_3O_{7-\delta}$ nanorings to probe fluxoid quantization in High Critical Temperature Superconductors

R.Arpaia[a,b], S.Charpentier[a], R.Toskovic[a,c], T.Bauch[a], F.Lombardi[a,*]

[a] *Quantum Device Physics Laboratory, Department of Microtechnology and Nanoscience, Chalmers University of Technology, SE-41296 Göteborg, Sweden*
[b] *CNR-SPIN, Dipartimento di Scienze Fisiche, Università degli Studi di Napoli Federico II, I-80126 Napoli, Italy*
[c] *Department of Quantum Nanoscience, Kavli Institute of Nanoscience, Delft University of Technology, NL-2628 CJ Delft, The Netherlands*

Abstract

We have realized $YBa_2Cu_3O_{7-\delta}$ (YBCO) nanorings and measured the magnetoresistance $R(B)$ close to the superconducting transition. The large oscillations that we have measured can be interpreted in terms of vortex dynamics triggering the nanowires to the resistive state. The Fast Fourier Transform spectrum of the magnetoresistance oscillations shows a single sharp peak for nanorings with narrower loop arm width: this peak can be univocally associated to a $h/2e$ periodicity as predicted for optimally doped YBCO. Moreover it is a clear evidence of a uniform vorticity of the order parameter inside the rings, confirming a high degree of homogeneity of our nanostructures. This result gives a boost to further investigations of YBCO nanorings at different dopings within the superconducting dome, where in the underdoped regime a $R(B)$ periodicity different from the conventional $h/2e$ has been predicted.
Keywords: High-temperature superconductors, nanorings, fluxoid

*Corresponding author
Email address: floriana.lombardi@chalmers.se (F.Lombardi)

quantization, vortex dynamics

1. Introduction

Multiply-connected structures like cylinders and rings are the basic structures for studying a variety of quantum mechanical effects, including the fluxoid quantization [1, 2, 3, 4]. These structures have attracted a lot of interest in the last few years, after theoretical studies have predicted the appearance of an additional h/e component in the magnetoresistance of nanorings made by High Critical Temperature Superconductors (HTS), associated with the d-wave symmetry of the order parameter [5, 6, 7, 8, 9]. At the same time, theories based on a charge stripe order, to explain the microscopic mechanism for HTS, have predicted the appearance of a $h/4e$ periodicity (corresponding to half a quantum of flux), replacing/coexisting with the usual periodicity of $h/2e$ [10]. The analysis of the magnetoresistance $R(B)$ oscillations, which can be observed in nanorings at temperatures close to the superconducting critical temperature T_C (Little-Parks effect), allows the identification of the charge of the carrier responsible for the superconducting phenomenon. In the case of HTS, these measurements can shed light on the HTS pairing mechanisms. Magnetoresistance measurements made on HTS nanorings [11, 12], and in particular on $YBa_2Cu_3O_{7-\delta}$ (YBCO) submicron rings [13], have shown, up to now, that in the optimally doped regime only the periodicity $h/2e$ is present.

However, the various theories for the microscopic mechanism of HTS give the sharpest predictions in the underdoped regime. The study of fluxoid quantization in HTS nanorings as a function of doping remains an impor-

tant tool to discriminate among the various theoretical approaches, where a crossover from $h/2e$ to h/e or $h/4e$ flux periodicities is predicted [14]. An important step in this field is the realization of nanorings with homogeneous superconducting properties close to the as grown films. In this way any new periodicity possibly detected in the magnetoresistance oscillations can be univocally associated to a different elemental charge carrier (compared to the conventional $2e$ Cooper pair) or to new effects related to the d-wave symmetry of the order parameter.

In this contribution we report on recent developments in the fabrication and measurement of YBCO nanorings, where the superconducting properties are uniform across the arms of the nanorings down to dimensions of the order of 50 nm.

The nanorings are made of nearly optimally doped YBCO, with cross sections down to 50×30 nm^2, using an improved nanopatterning procedure described in Refs. [15, 16, 17]. As a consequence of the soft ion milling procedure and of the presence of a Au capping layer on top of the nanowires, we have achieved YBCO nanostructures, demonstrating "pristine" superconducting properties, characterized by a critical current density close to the theoretical Ginzburg-Landau depairing limit [18].

2. Nanoring fabrication and design

The devices have been realized by patterning 30 nm thick YBCO films, provided by Theva GmbH, grown on MgO (001) substrates and with a T_C of 85 K. Details on the nanopatterning procedure can be found elsewhere [15, 18]. Fig. 1(a) shows the typical ring geometries we have realized: the

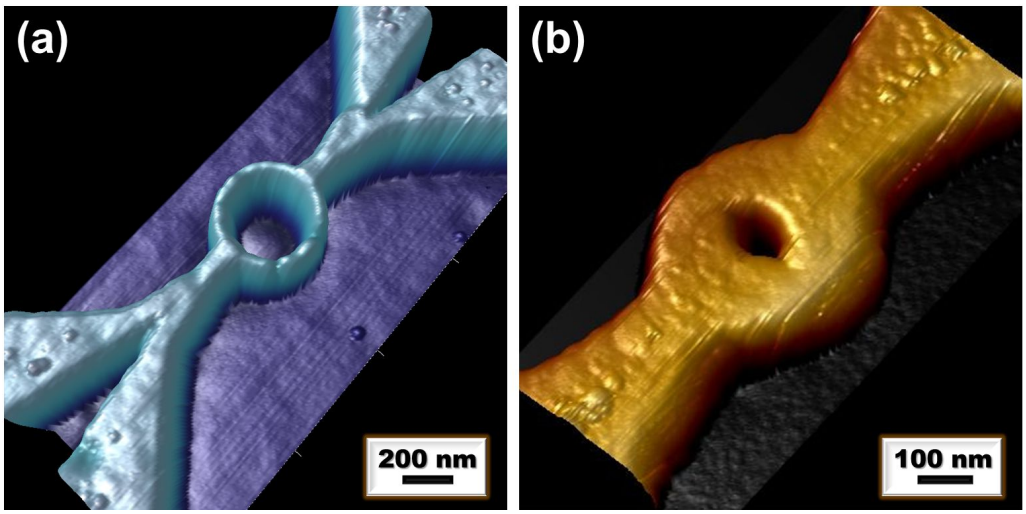

Figure 1: (a) AFM picture of a typical 30 nm thick nanoring, with internal radius of 150 nm and a linewidth of 50 nm. (b) AFM picture of a wider nanoring (w = 160 nm), used for comparison.

rings have the internal radius r_{int} in the range 120-200 nm, and the arm width w is in the range 50-80 nm. The four wide electrodes, used as current and voltage probes during the measurements, are situated very close to the nanostructures. For our geometries we have made numerical calculations of the current density across the nanorings to evaluate the effective area A_{eff}, following Refs. [19, 20], which is fundamental to determine the flux across the ring and therefore the periodicity of the magnetoresistance oscillations. The values we have obtained are in very good agreement with those of the geometrical area of the ring $A_g = \pi r_{avr}^2$, with $r_{avr} = r_{int} + (w/2)$ being the average radius.

For comparison, we have also fabricated a few wider rings, with arm width w in the range 150-200 nm (see Fig. 1(b)).

3. Magnetoresistance measurements

Resistance vs Temperature $R(T)$ and magnetoresistance $R(B)$ measurements of different nanorings have been carried out in a Physical Property Measurement System (PPMS) of Quantum Design with a temperature stability of about ± 1 mK, using a 4-point measurement scheme. In the following, we will focus on the nanoring shown in Fig. 1(a), which exhibits the typical characteristics of most of the devices we have measured.

Fig. 2(a) shows the $R(T)$ curve. Since the electrodes are closely attached

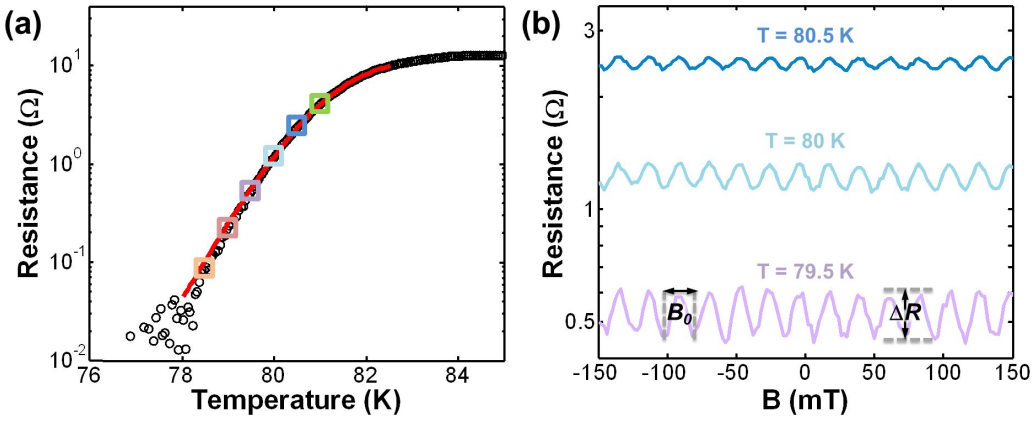

Figure 2: (a) $R(T)$ curve of the ring shown in Fig. 1(a), obtained by biasing the ring with a 500 nA current. The red solid line is the fit to the data, obtained assuming assuming a vortex-dynamics model. (b) On the $R(T)$ transition, at fixed values of the temperature, we have applied an external magnetic field, observing large magnetoresistance oscillations (which are reported here for three different temperatures).

to the nanostructure, only the transition related to the nanoring is observed. The broadening of the resistive transition can be fitted in terms of a vortex slip model [21], considering the actual dimensions measured by AFM: we

have extracted feasible values for λ_0 and ξ_0 ($\lambda_0 \approx 340$ nm and $\xi_0 \approx 2.5$ nm), only slightly higher than those we have obtained from nanowires with similar widths [18], which is possibly related to the thinner YBCO layer [22]. This result highlights the high quality of our nanostructures even with cross sections as small as 50×30 nm^2.

We have measured the magnetoresistance of the ring at different temperatures within the resistive transition (see colored opened squares in Fig. 2(a)). Large oscillations appear as a function of the flux enclosed by the ring (see Fig. 2(b)). Considering the geometrical area of the ring $A = \pi r_{avr}^2$, with $r_{avr} = 175$ nm, and the magnetic field periodicity $B_0 = 22$ mT, we have that the flux periodicity $\Phi = B_0 \pi r_{avr}^2$ is equal to Φ_0, in agreement with a conventional $h/2e$ quantization.

Oscillations of the resistance as a function of the externally applied magnetic field are observed in the range $78 - 82$ K. The temperature dependence of the amplitude of these oscillations, ΔR, is shown in Fig. 3(a) (colored circles).

The most straightforward interpretation for these oscillations is the Little-Parks effect [3, 23]. According to this model, the expected temperature oscillations should have an amplitude $\Delta T_C = 0.14 T_C (\xi_0/r_{avr})^2 \approx 1.5$ mK, with $T_C \approx 82$ K, defined at the onset of the superconducting transition, and $\xi_0 \approx 2$ nm. Since in the actual experiments one measures the resistance oscillations as a function of H rather than ΔT_C, it is possible to calculate the upper limit of the resistance amplitude predicted by the Little-Parks effect via the expression $\Delta R = \Delta T_C (\mathrm{d}R/\mathrm{d}T)$. The grey dashed line in Fig. 3(a) shows the expected Little-Parks ΔR. The discrepancy between the measured

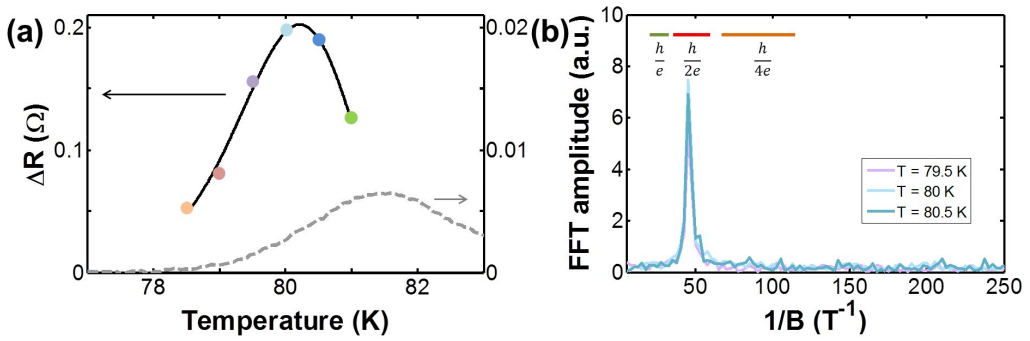

Figure 3: (a) Amplitude ΔR of the R(B) oscillations of Fig. 2, at different temperatures (points). The solid line represents the fit of the data by using eq. (1), accounting for the interaction between thermally excited moving vortices and oscillating screening currents circulating in the two arms of the ring. The dashed line represents instead an upper limit for the amplitude of the resistance oscillations as predicted by the Little-Park effect (its scale, on the right, is expanded by a factor 10). (b) FFT of the three R(B) curves shown in Fig. 2(b). The h/e, $h/2e$ and $h/4e$ bars indicate the 1/B (frequency) range calculated from ring sizes (the ends of each bar correspond to the internal and external radius of the ring), and assuming h/e, $h/2e$ and $h/4e$ flux periodicity, respectively (see more comments in note 1).

resistance amplitudes ΔR and those predicted by the Little-Parks effect is more than a factor 10.

These large magnetoresistance oscillations, which cannot be ascribed to classic Little-Parks oscillations, have been already observed in HTS nanoloops [11, 24] and explained in terms of the vortex dynamics, triggering the resistive state in 3-dimensional nanowires. The analysis of the $R(T)$ curve of our nanoring confirms this scenario, since we have successfully fitted the resistive transition within the vortex-dynamics model. The energy barrier for vortex entry [25] is oscillatory, as a consequence of the interaction of the thermally

excited moving vortices with the screening current circulating in the two arms of the ring, which is a periodic function of the externally applied magnetic field. The equation describing the temperature dependent amplitude of the magnetoresistance oscillations is [11]:

$$\Delta R \approx R_0 \Big(\frac{\epsilon_0^r}{2k_B T} \Big)^2 \frac{K_1(\gamma)}{(K_0(\gamma))^3} \ , \tag{1}$$

where $\epsilon_0^r = \Phi_0^2 w/(4\pi\sqrt{\pi} r_{avr} \mu_0 \lambda_P(T))$ is the characteristic energy of a vortex in a nanoring, $\lambda_P(T) = \lambda_L^2(T)/t$ the Pearl length, t the thickness of the ring arms, R_0 the resistance at the onset of the superconducting transition, K_0 and K_1 the zero-order and first-order modified Bessel functions of the first kind respectively and $\gamma = (E_\nu + E_0/4)/(2k_B T)$, with $E_\nu = (\Phi_0^2/(4\pi\mu_0\lambda_P(T)))\ln(2w/(\pi\xi(T)))$ the energy barrier for vortex entry, in the limit of zero bias. We have fitted the measured $\Delta R(T)$ with eq. (1), by using λ_0 and ξ_0 as fitting parameters. As shown by the solid line in Fig. 3(a), the agreement between the data and the model is excellent, and the values of $\lambda_0 \approx 360$ nm and $\xi_0 \approx 3$ nm, which we extract, are in agreement with those extracted from the fitting of the $R(T)$. The magnetoresistance oscillations originate from both the vortex dynamics and from the Little-Parks effect. In our case, the contribution of the vortex dynamics is dominant, as a consequence of the strong thermal fluctuations; at the same time, the contribution of the Little-Parks effect is very small, because of the short coherence length in YBCO.

To further analyze the magnetoresistance oscillations, the Fast Fourier Transform (FFT) method has been used. In Fig. 3(b) the FFT spectra are shown, as a function of the temperature. The FFT peak at 46 T^{-1} corresponds to a loop with radius $r = 175$ nm, which coincides with the r_{avr}

extracted by AFM. The FFT analysis also allows the following considerations:

- Only one sharp peak in the FFT is present, associated to a $h/2e$ periodicity. In previous experiments on YBCO nanorings, additional unexpected peaks were observed [13]. They have been associated to the presence, within the ring arms with $w \gg \xi$ ($w \approx 270 - 300$ nm), of different characteristic radii, with a spacing of $20 - 30$ nm, characterized by a different value of the order parameter vorticity (superfluid momentum). In our case, a uniform vorticity is present, mainly as a consequence of the high homogeneity of the superconducting properties in the nanoring arms.

- The FFT peak position, corresponding to the value of the ring average radius, is constant as a function of the temperature, even at temperatures very close to T_C. This result proves that all the regions within the ring show the same T_C and there are no subdomains with depressed superconducting properties induced by damages during the nanopatterning.

- The peak in the FFT spectra can be unequivocally determined and associated to the $h/2e$ periodicity, since there is no overlapping between the frequency ranges associated to different possible periodicities (h/e, $h/2e$, $h/4e$). Indeed, because of the finite width of the ring arms, the periodicity of the resistance oscillations in B is associated to a certain frequency range, whose extremes are given by r_{int} and $r_{ext} = r_{int}+w$. If different frequency ranges (corresponding to different fluxoid quantization) are compatible with the FFT peak, the determination of

the fluxoid value is uncertain. This ambiguity is overcome if the arm width w fulfills the condition[1]

$$w \leq r_{int}(\sqrt{2}-1)\ . \tag{2}$$

To highlight the importance of using nanorings with very narrow arms, we have also characterized few "wide" nanorings, not fulfilling the requirement of eq. 2 on the arm linewidth. In Fig. 4 the main results are summarized. In this case the large magnetoresistance oscillations, we have measured on

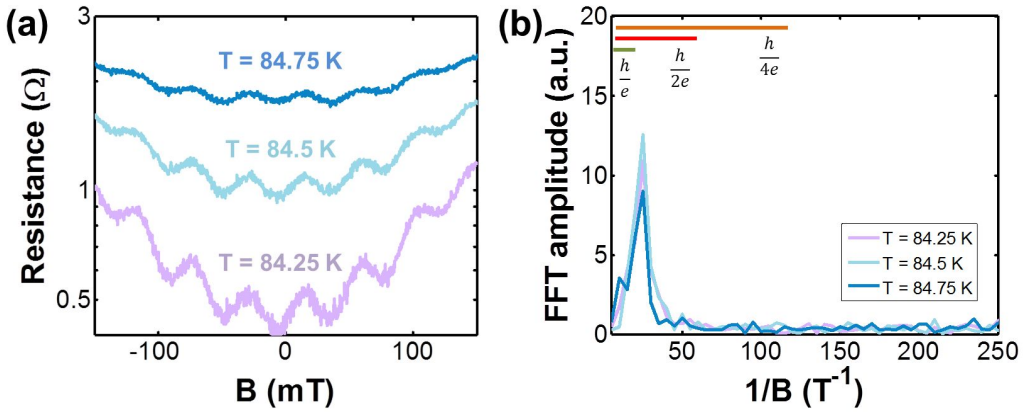

Figure 4: (a) R(B) oscillations of the "wide" ring of Fig. 1(b), measured at three different temperatures. (b) FFT of the three curves of panel (a), after the subtraction of the parabolic-like background.

the resistive transition, are superimposed to a parabolic-like background (see

[1]The extremes of each frequency range are $f^i_{min} = 1/B^i_{max} = \pi r^2_{int}/\Phi^i_0$ and $f^i_{max} = 1/B^i_{min} = \pi r^2_{out}/\Phi^i_0$, with $r_{out} = r_{int} + w$ and $\Phi^i_0 = h/i, i = e, 2e, 4e$, depending on the considered frequency range. The conditions to avoid overlapping between different frequency ranges are $f^e_{max} < f^{2e}_{min}$ and $f^{2e}_{max} < f^{4e}_{min}$. Substituting in these two equations the expressions for f_{max} and f_{min}, the condition (2) is found.

Fig. 4(a)). The origin of the parabolic-like background is related to the non-negligible width of the ring arms [11]. In such a case, at magnetic fields corresponding to integer numbers of the flux quanta the supercurrent density is zero only for $r = r_{avr}$, while flowing with different sign for radii smaller and larger than r_{avr} [26]. These local currents increase with the externally applied magnetic field, causing an additional reduction of the vortex entry barrier and hence a parabolic-like background in the $R(B)$ measurements. Fig. 4(b) shows the FFT spectrum, considering only the magnetic field range [-100 mT, 100 mT], where the subtraction of the parabolic-like background is more accurate. The peak at 22 T^{-1} corresponds to a loop radius $r = 120$ nm, which is fairly close to the AFM extracted average loop diameter $r_{avr} = 115$ nm. For wider rings (as in Fig. 4(b)) the FFT amplitude of the main peak is wider than that of narrower rings (as in Fig. 3(b)), mainly as a consequence of the reduced number of oscillations (≈ 4). The smaller geometrical area of the loop in wider rings causes a larger oscillation period, introducing at the same time complications in the analysis at high magnetic field, because of the appearance of the parabolic-like background. For instance, the shoulder in the FFT peak at low frequencies is an artifact, due to the subtraction of the background. Finally, for wider cross sections, the frequency ranges corresponding to the three possible periodicities, related to a flux quantum h/e, $h/2e$ or $h/4e$, overlap. This makes the association of the peak at 22 T^{-1} in the FFT to a specific value of the flux quantum in principle not unequivocal[2].

[2]From the analysis done on the narrower ring in Fig. 3(b), we can associate this peak to a $h/2e$ flux periodicity.

4. Conclusions

In conclusion, we have fabricated nanorings made of nearly optimally doped YBCO, with cross sections down to 50×30 nm^2. Resistance vs Temperature $R(T)$ curves present a broadening in the transition around T_C, that we have nicely fitted with a vortex-dynamics model. Magnetoresistance $R(B)$ measurements close to T_C show large oscillations that cannot be attributed to the Little-Parks effect. The temperature dependence of the amplitude of these oscillations can instead be interpreted considering the modulation of the height of the energy barrier for vortex entry, driven by the external magnetic field. A single sharp peak characterizes the Fast Fourier Transform spectrum of the magnetoresistance oscillations of nanorings with narrower linewidth: this peak, associated to $h/2e$ periodicity, confirms the $2e$ value for the elemental superfluid charge in optimally doped YBCO. Moreover, it represents a clear evidence of a uniform vorticity of the order parameter inside the rings, which is a consequence of the high degree of homogeneity of these nanostructures. These results represent solid grounds for future experiments on underdoped YBCO nanorings and on nanorings with various YBCO orientations [27], where different values of the fluxon might be detected.

Acknowledgements

This work has been partially supported by the Swedish Research Council (VR) and the Knut and Alice Wallenberg Foundation. Riccardo Arpaia was partially supported by a grant from the Foundation BLANCEFLOR Boncompagni Ludovisi, née Bildt.

References

[1] Y. Aharonov, D. Bohm, Phys. Rev. 115 (1959) 485–491.

[2] M. Grochol, F. Grosse, R. Zimmermann, Physical Review B 74 (2006) 115416.

[3] W. A. Little, R. D. Parks, Phys. Rev. Lett. 9 (1962) 9–12.

[4] N. C. Koshnick, H. Bluhm, M. E. Huber, K. A. Moler, Science 318 (2007) 1440–1443.

[5] V. Juričić, I. F. Herbut, Z. Tešanović, Phys. Rev. Lett. 100 (2008) 187006.

[6] F. Loder, A. P. Kampf, T. Kopp, J. Mannhart, C. W. Schneider, Y. S. Barash, Nature Physics 4 (2008) 112–115.

[7] V. Vakaryuk, Phys. Rev. Lett. 101 (2008) 167002.

[8] T.-C. Wei, P. M. Goldbart, Phys. Rev. B 77 (2008) 224512.

[9] J.-X. Zhu, H. T. Quan, Phys. Rev. B 81 (2010) 054521.

[10] E. Berg, E. Fradkin, S. A. Kivelson, Nature Physics 5 (2009) 830–833.

[11] I. Sochnikov, A. Shaulov, Y. Yeshurun, G. Logvenov, I. Bozovic, Nature Nanotechnology 5 (2010) 516–519.

[12] F. Tafuri, D. Massarotti, L. Galletti, D. Stornaiuolo, D. Montemurro, L. Longobardi, P. Lucignano, G. Rotoli, G. Pepe, A. Tagliacozzo, F. Lombardi, Journal of Superconductivity and Novel Magnetism 26 (2013) 21–41.

[13] F. Carillo, G. Papari, D. Stornaiuolo, D. Born, D. Montemurro, P. Pingue, F. Beltram, F. Tafuri, Phys. Rev. B 81 (2010) 054505.

[14] F. Carillo, G. M. De Luca, D. Montemurro, G. Papari, M. Salluzzo, D. Stornaiuolo, F. Tafuri, F. Beltram, New Journal of Physics 14 (2012) 083025.

[15] R. Arpaia, S. Nawaz, F. Lombardi, T. Bauch, IEEE Trans. Appl. Supercond. 23 (2013) 1101505.

[16] S. Nawaz, R. Arpaia, F. Lombardi, T. Bauch, Phys. Rev. Lett. 110 (2013) 167004.

[17] R. Arpaia, M. Ejrnaes, L. Parlato, R. Cristiano, M. Arzeo, T. Bauch, S. Nawaz, F. Tafuri, G. P. Pepe, F. Lombardi, Supercond. Sci. Technol. 27 (2014) 044027.

[18] S. Nawaz, R. Arpaia, T. Bauch, F. Lombardi, Physica C 495 (2013) 33 – 38.

[19] J. R. Clem, E. H. Brandt, Phys. Rev. B 72 (2005) 174511.

[20] R. Arpaia, M. Arzeo, S. Nawaz, S. Charpentier, F. Lombardi, T. Bauch, Appl. Phys. Lett. 104 (2014) 072603.

[21] R. Arpaia, D. Golubev, R. Baghdadi, M. Arzeo, G. Kunakova, S. Charpentier, S. Nawaz, F. Lombardi, T. Bauch, Physica C (2014).

[22] A. G. Zaitsev, R. Schneider, G. Linker, F. Ratzel, R. Smithey, P. Schweiss, J. Geerk, R. Schwab, R. Heidinger, Rev. Sci. Instrum. 73 (2002) 335–344.

[23] R. D. Parks, W. A. Little, Phys. Rev. 133 (1964) A97–A103.

[24] D. Levi, A. Shaulov, A. Frydman, G. Koren, B. Y. Shapiro, Y. Yeshurun, Europhysics Letters 101 (2013) 67005.

[25] L. N. Bulaevskii, M. J. Graf, C. D. Batista, V. G. Kogan, Phys. Rev. B 83 (2011) 144526.

[26] V. G. Kogan, J. R. Clem, R. G. Mints, Phys. Rev. B 69 (2004) 064516.

[27] J. Johansson, K. Cedergren, T. Bauch, F. Lombardi, Phys. Rev. B 79 (2009) 214513.